Heliyon 10 (2024) e38263

Contents lists available at ScienceDirect

Heliyon

journal homepage: www.cell.com/heliyon

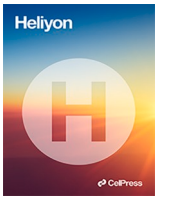

Research article

WDR64, a testis-specific protein, is involved in the manchette and flagellum formation by interacting with ODF1

Yunfei Zhang [a,b], Xiaowei Xing [b], Lihua Huang [b], Yuyan Su [a,b], Gang Liu [c], Xinxing Zhang [b], Youbo Yang [d,*]

[a] Department of Laboratory Medicine, the Third Xiangya Hospital, Central South University, Changsha, China
[b] Center for Experimental Medicine, the Third Xiangya Hospital, Central South University, Changsha, China
[c] The Institute of Reproduction and Stem Cell Engineering, Central South University, Changsha, China
[d] Department of Endocrinology, the Third Xiangya Hospital, Central South University, Changsha, China

ARTICLE INFO

Keywords:
WDR64
Testis-enriched gene
ODF1
Protein interaction
Sperm flagellum

ABSTRACT

The WD40 repeat (WDR) domain is present in a wide range of proteins, providing sites for protein–protein interactions. Recent studies have shown that WDR proteins play indispensable roles in spermatogenesis, such as in spermatocyte division, sperm head formation and flagellar assembly. In this study, we identified a novel testis-specific gene, *WDR64*, which has the typical characteristics of WD40 proteins with two β-propellers, and is highly conserved in Mammalia. RT-PCR and Western blot results revealed that *WDR64* was highly expressed in testis. WDR64 protein was weakly expressed at postnatal Day 7, increased substantially at postnatal Day 28 and maintained at high levels thereafter. Further immunofluorescence demonstrated that WDR64 was localized posterior to the nucleus in steps 8–14 spermatids in line with the dynamic localization of manchette, moved to the flagella in steps 15–16 spermatids, and localized at the midpiece of the flagellum in mature spermatozoa. To explore the function of WDR64, we performed immunoprecipitation–mass spectrometry (IP–MS) to screen its interacting proteins and found that WDR64 interacted with ODF1 to form a complex. The WDR64/ODF1 complex is located at the manchette during nucleus shaping and finally at the midpiece of the mature spermatozoa tail, suggesting that it may be involved in the assembly of the manchette and flagella during spermiogenesis. Our findings provide the first understanding of the expression pattern of WDR64 and its potential molecular mechanism in spermiogenesis.

1. Introduction

Human infertility has become a global reproductive health problem. It is estimated to affect approximately 10–15 % of couples of reproductive ages, and male factors contribute to 30–50 % of cases of infertility [1,2]. It is widely recognized that genetic factors are likely involved in a large proportion of male infertility [3,4]. The genetic landscape of male infertility is extremely complex since testis histological phenotypes are heterogeneous, and at least 2000 genes are involved in spermatogenesis [5]. However, the functions of a considerable number of genes are not well understood.

WD40 repeat (WDR) proteins are prevalent in all eukaryotes and act as scaffold proteins to form molecular "hubs" for protein–DNA

* Corresponding author.
E-mail address: yangyoubo@126.com (Y. Yang).

https://doi.org/10.1016/j.heliyon.2024.e38263
Received 4 July 2024; Received in revised form 20 September 2024; Accepted 20 September 2024
Available online 21 September 2024

or protein–protein interactions [6]. The WD motif is characteristic of 40–60 amino acids with conserved tandem tryptophan and aspartic acid (WD) repeats at the C-terminus and glycine/histidine (GH) residues at 11–24 amino acids downstream from the N-terminus [7]. The WD40 repeat domains typically fold into seven-bladed β-propeller structures with a donut-like shape [8]. More than 360 WDR proteins have been annotated and these proteins are involved in a broad range of biological functions, including DNA damage sensing and repair, epigenetic regulation of gene expression and chromatin organization, cell cycle regulation, signal transduction, and cilia and flagella assembly pathways [8–10].

In recent years, increasing evidence has shown that the WDR protein family plays an indispensable role in gametogenesis. *Wdr62* is associated with the meiosis of germ cells. The knockout of *Wdr62* in mice led to defective initiation of meiosis in female germ cells and metaphase meiosis arrest in male germ cells due to abnormal spindle assembly [11–13]. Cullin-RING E3 ubiquitin ligase (CRL)-4 (*DCAF8*, also known as *WDR42A*) and *WDR12* play critical roles in head formation during spermiogenesis [14,15]. *Dcaf8* knockout mice presented a pronounced increase in morphologically abnormal sperm with typical bent head malformation and significantly reduced fertilization rate [14]. *WDR12* homozygous mutation in men led to tapered-head spermatozoa [15]. In addition, the cilia-and flagella-associated protein 43 (CFAP43, also known as WDR96), CFAP44 (WDR52), CFAP251 (WDR66) and WDR63 proteins are thought to be related to the formation of sperm flagella, and deficiency of these genes in humans and mice can cause multiple morphological abnormalities of sperm flagella (MMAF) and male infertility [16–20]. Recently, our group has explored the function of WDR proteins in spermatogenesis. We demonstrated that WDR87 is highly expressed in testes and interacts with CFAP47 to form a complex that participates in in the spermatozoa tail assembly, and that the expression of WDR87 is significantly decreased in patients with *CFAP47* mutation [21]. WDR38, another WDR protein, is a novel equatorial segment protein and that interacts with RAB19 and GM130, playing roles in acrosome biogenesis [22]. However, the functions of many WDR proteins in spermatogenesis have not yet been explored.

Recently, we analyzed WDR genes with testis-specific expression and found that 12 WDR genes were enriched in the clusters. However, the function of *WDR64* is still unknown. The WDR64 protein, a member of the WDR protein family, has a molecular weight of approximately 124 kDa and contains 14 WD40 motifs. In the present study, we investigated the characteristics, expression profile and cellular localization of WDR64, and its interaction with ODF1 to elucidate its potential function in spermiogenesis.

2. Materials and methods

2.1. Animals

The animal experiments were approved by the Experimental Animals Ethics Committee of Central South University. C57BL/6J mice were raised in the specific pathogen-free (SPF) animal facility of the Department of Laboratory Animals of Central South University, provided with standard food and bacteria-free water and were kept with a 12 h–12 h light–dark cycle at 18–22 °C and 50–60 % humidity. All the operations followed the relevant animal ethics regulations.

2.2. Bioinformatics analysis

The structure of human WDR64 was predicted by AlphaFold2 and visualized in PyMOL [23]. Amino acid multiple sequence alignment of WDR64 from different species was performed using MAGEX and Clustal, and the results were visualized in ESPript3.0 [24,25]. The expression of human *WDR64* in different tissues was predicted based on online data from the Human Protein Atlas.

The analyses of published single-cell RNA sequencing datasets were performed using the Sperm Maturation Database (SperMD) [26]. We evaluated the expression of WDR64 in single-cell RNA sequencing datasets by Guo et al. [27,28] (GEO: GSE120508 and GSE134144 for human testis), Leir et al. [29] (GEO: GSE148963 for human epididymis), Chen et al. [30] (GEO: GSE107644 for mouse testis), and Shi et al. [31] (GEO: GSE159713 for mouse epididymis).

Analyses of the protein–protein docking model were performed by using GRAMM-X to investigate the relationship between WDR64 and ODF1. PyMOL and PDBePISA were used to investigate and visualize the protein–protein interactions.

2.3. Construction of plasmids, cell culture and transfection

Testis cDNA from 8-week wild-type (WT) mice was used as the template for the construction of plasmids. The full-length open reading frame (ORF) of *Wdr64* cDNA (GenBank NM_029453.2) tagged with Flag was cloned and inserted into the *EcoRI*/*Not*I sites of the pLVX-IRES-Puro vector, and the assembled construct was termed pLVX-Flag-Wdr64. The inserted fragment was verified by Sanger sequencing. For transient transfection, the HEK293T cells were maintained in Dulbecco's minimal essential medium (DMEM) supplemented with 10 % fetal bovine serum (FBS). Cells in the rapid growth phase were transfected using Lipo 8000™ Transfection Reagent (Beyotime, China). After 48 h, the cells were harvested for Western blotting.

2.4. RNA isolation and RT–qPCR

Total RNA from different tissues from 8-week-old WT mice and testes from different day-old mice was extracted using TRIzol reagent (Thermo Fisher, USA). The concentrations of RNAs were measured with a NanoDrop nucleic acid analyzer. The first complementary DNA (cDNA) strand was synthesized according to the instructions of the HiScript II Q RT SuperMix (Vazyme, China). The cDNA was subsequently used for quantitative RT–PCR with ChamQ Universal SYBR qPCR Master Mix (Vazyme, China) on a

LightCycler 480 Real-Time PCR instrument (Roche, Switzerland) according to the manufacturer's instructions. The comparative ΔCt (cycle threshold) method was used to analyze the qRT−PCR data for calculating the relative gene expression levels. The primers used for qPCR are listed in Supplementary Table S1.

2.5. Western blotting

HEK293T cells transfected with control or pLVX-Flag-Wdr64 plasmids were lysed in RIPA buffer supplemented with protease inhibitor. Different tissues collected from 8-week-old wild-type (WT) mice and testis tissues collected from WT mice at different developmental stages were ground and lysed. The collected supernatants were separated by 8 % SDS−PAGE (Biosharp, China) and transferred onto polyvinylidene fluoride (PVDF) membranes (Millipore, USA). After blocking with 5 % nonfat milk, the membranes were incubated at 4 °C overnight with the following antibodies: mouse anti-Flag monoclonal antibody (66008-4-Ig, Proteintech, China), rabbit anti-ODF1 monoclonal antibody (ab197029, Abcam, USA), rabbit anti-WDR64 polyclonal antibody (PA5-49160, Thermo Fisher, USA), and mouse anti-GAPDH monoclonal antibody (60004-1-Ig, Proteintech, USA). The membranes were subsequently washed with TBST (1 × TBS containing 0.1 % Tween-20) three times and incubated with the corresponding secondary antibodies conjugated with horseradish peroxidase for 1 h. After washing three times, an enhanced chemiluminescence kit (Biosharp, USA) was used to visualize the protein bands with a UVP ChemStudio PLUS multifunctional imager (UVP, USA).

2.6. Immunofluorescence assay

For the preparation of testicular cell smears, the sheared testis was filtered through a 200-mesh sieve and washed with PBS at least three times. The cells were collected, fixed with 4 % paraformaldehyde and smeared on lysine-coated glass slides. The testicular cell smears were subsequently permeabilized with 0.5 % Triton X-100 and blocked with 5 % bovine serum albumin (BSA). The slides were hybridized with primary antibodies overnight at 4 °C. After three washes, hybridization with the corresponding fluorescent secondary antibodies or peanut agglutinin (PNA), incubation with DAPI, and glycerol sealing, the fluorescence-stained cells were observed under a fluorescence microscope (Zeiss, Germany).

For the staining of testis sections, the mouse testes were fixed with 4 % paraformaldehyde at 4 °C for 24 h and then paraffin-embedded after dehydration with ethanol. The testes were cut to sections with thickness of 5 μm, and the sections were deparaffinized, incubated in sodium citrate buffer at 95 °C for 20 min and blocked with 5 % BSA. Subsequently, immunofluorescence staining was routinely performed and the results were visualized.

2.7. Coimmunoprecipitation (Co-IP)

The malignant human testis pluripotent embryonic carcinoma NT2/D1 cells or testes from 8-week-old WT mice were lysed with 1 ml of IP Lysis/Wash Buffer of Classic Mag IP/Co-IP Kit (Thermo Fisher, USA) supplemented with phosphatase inhibitors for 20 min. After centrifugation at 12,000 rpm at 4 °C for 25 min, the supernatant was collected and divided into 400 μL for each IP group and 200 μL for input. Each IP group contained 4 μg of target antibodies or mock antibodies (IgG) and was incubated with rotation at 4 °C overnight. The antibody−protein complex was subsequently, bound with 25 μL of Protein A/G-coated magnetic beads (Thermo Fisher, USA) to form protein−antibody−bead complexes for 8 h at 4 °C on a rotator. Finally, the immunoprecipitated proteins were eluted for subsequent sodium dodecyl sulfate−polyacrylamide gel electrophoresis (SDS−PAGE) and Western blot analysis.

2.8. Silver staining and mass spectrometry (MS)

Silver staining of the SDS−PAGE gel was performed using a Fast Silver Stain Kit (Beyotime, China) according to the manufacturer's instructions. Briefly, the SDS−PAGE gel was fixed in a solution of ethanol:glacial acetic acid:water (50:10:40) for at least 40 min. After being washed with 30 % ethanol and water, the gel was incubated in sensitizing buffer for 2 min. After being washed for two times, the gel was then stained in silver solution and visualized. Mass spectrometry analysis of the silver-stained gel was performed with an EASY-nLC system (Thermo Fisher, USA).

2.9. Data analysis

The data are presented as the means ± standard deviations (SDs) and graphs were generated using GraphPad PRISM version 8. All the data shown in the study were obtained from at least three independent experiments.

3. Results

3.1. WDR64 is a testis-enriched gene

WDR proteins are often essential for constituting one of the most abundant protein−protein interaction complexes, and are involved in a broad range of biological functions [6,9]. According to the classification method of testis-enriched genes by Chang et al. [32], we analyzed the WDR genes and found that 12 WDR genes were classified as high-confidence testis-enriched genes (Fig. 1A). Further analysis of these testis-enriched WDR genes showed that *DCAF12L1* (*WDR40B*) is involved in azoospermia in men, but loss of

Dcaf12l1 in mice is dispensable for male infertility [33]; *DCAF4L1* (*WDR21B*), *DCAF4L2* (*WDR21C*) and *FBXW10* are cancer susceptibility factors [34–36]; *DCAF4L2* (*WDR21C*) is associated with cleft lip [37]; *DCAF8L1* (*WDR42B*) and *TBL2* (*WBSCR13*) are involved in endocrine disorders [38,39]; *Dtl* (human *DCAF2*) knockout in mouse oocytes leads to female infertility, and *Dtl* conditional knockout in mice leads to embryonic death [40,41]; depletion of *Lrwd1* (human *LRWD1*) leads to retarded postnatal growth [42]; *WDR62* (*C19orf14*) regulates the process of neural stem cell and germ cell meiosis and is associated with the primary microcephaly and male infertility [43,44]; *WDR87* participates in sperm tail assembly and is also associated with recessive pediatric cataract [21]; and, *WDR88* is a susceptibility allele for schizophrenia [45]. Only *WDR64* has not yet been studied, thus we further investigated the

A

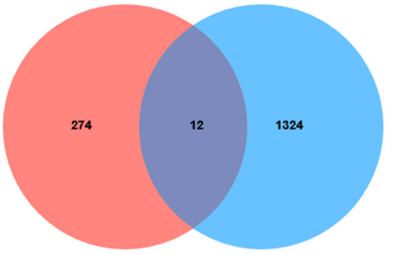

B

Genes	Model	Phenotype
DCAF12L1 (WDR40B)	Human and mice	Associated with azoospermia in men; but not essential for male fertility in mice
DCAF4L1 (WDR21B)	Human	Associated with hemangioblastomas
DCAF4L2 (WDR21C)	Human	Associated with orofacial cleft
DCAF8L1 (WDR42B)	Human	Overweight/obesity-associated gene
DTL (DCAF2)	Mice	Prolonged DNA replication and accumulation of massive DNA damage in oocytes; female infertility
FBXW10	Human and mice	Promoting factors of hepatocarcinogenesis
LRWD1	Mice	Retarded postnatal growth
TBL2 (WBSCR13)	Human	Associated with hyper-low-density lipoprotein cholesterolemia
WDR62 (C19orf14)	Human and mice	Primary microcephaly and premature ovarian insufficiency; oligoasthenoteratospermia
WDR64	-	-
WDR87	Human and mice	Associated with pediatric cataract ;participated in sperm tail assembly
WDR88	Human	Associated with schizophrenia

C

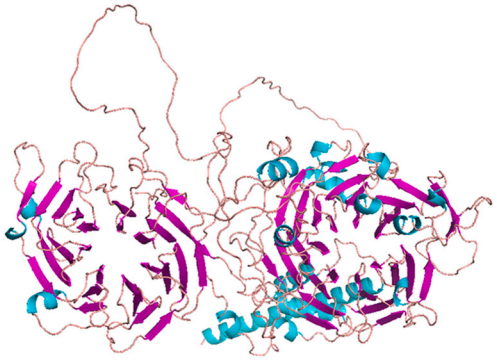

D

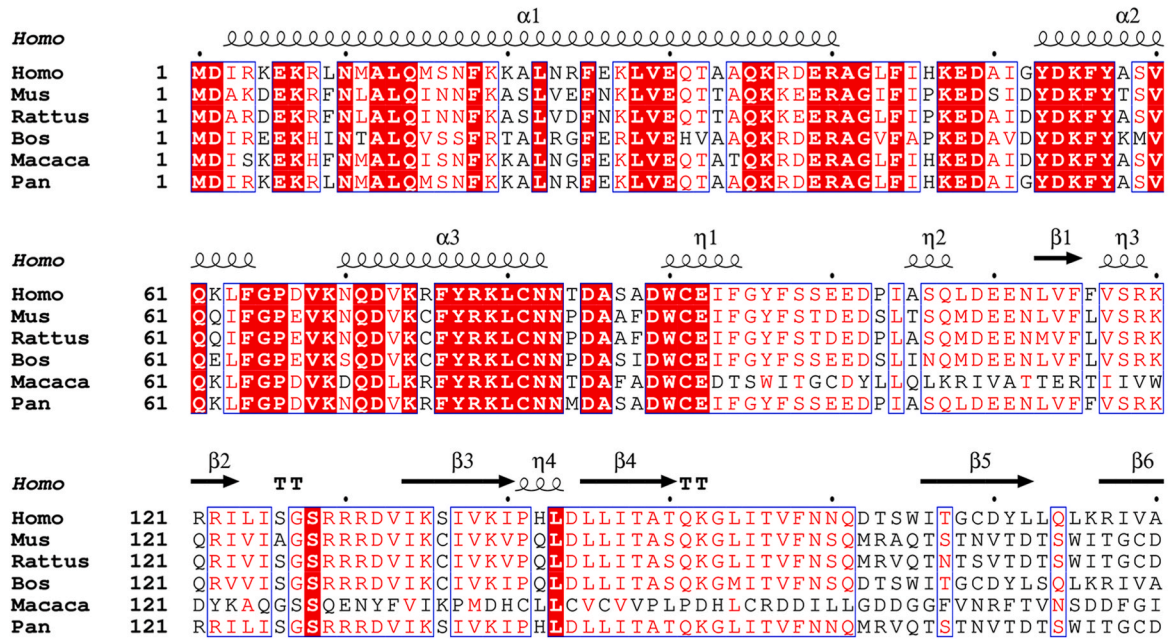

Fig. 1. Structural characteristics and conservation of WDR64. (A) Venn diagram showing the overlap between WDR genes and testis-enriched genes. (B) Phenotypes of overlapping genes between WDR genes and testis-enriched genes. (C) Schematic of the overall structure of the human WDR64 protein. (D) Multiple sequence alignment of WDR64 proteins from different species.

characteristics of *WDR64* (Fig. 1B).

To clarify the characteristics of *WDR64*, we used AlphaFold2 to predict the structure of the human WDR64 protein, and found that WDR64 has 14 WD repeats to form typical characteristics of WD40 proteins with two β-propellers, which are composed of every seven blades (Fig. 1C). Mmultiple sequence alignment analysis revealed that WDR64 is highly conserved from human (*Homo sapiens*) to chimpanzee (*Pan troglodytes*) (Fig. 1D). These data revealed that WDR64 was a member of WDR protein family and was specifically enriched in testis, indicating that WDR64 may play a role in mammalian testes.

3.2. *WDR64 expression in the human testis*

To investigate the role of *WDR64* in the testis, we first analyzed its expression patterns. According to the Human Protein Atlas database, *WDR64* was enriched in human testes (Fig. 2A). A more precise determination of *WDR64* expression in distinct stages of germ cell differentiation was performed using the single-cell RNA sequencing datasets of human testes published by Guo et al. [27,28]

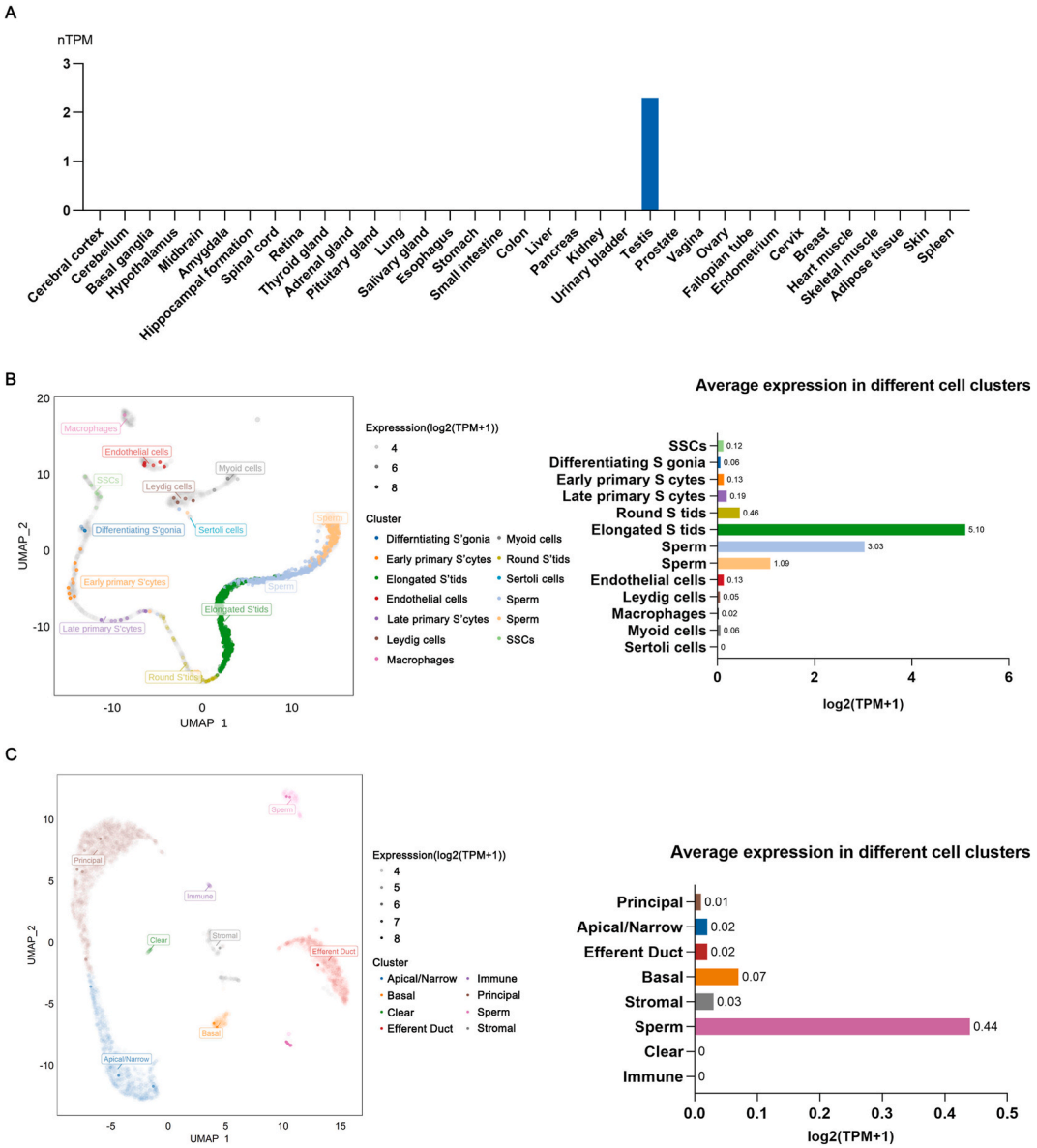

Fig. 2. Expression pattern of human *WDR64*. (A) RNA expression of human *WDR64* in the GTEx dataset. (B) Analysis of *WDR64* expression in the single-cell RNA dataset of human testis samples published by Guo et al. [27] Uniform manifold approximation and projection (UMAP) plots showing *WDR64* (left); the bar graph shows the average expression of *WDR64* in different cell clusters. (C) Analysis of WDR64 expression in the single-cell RNA dataset of testis samples from the human epididymis published by Leir et al. [29].

(Fig. 2B and Supplementary Fig. S1A). In detail, feature plots of *WDR64* expression revealed that *WDR64* was highly expressed in clusters of germ cells (Supplementary Fig. S1A), especially in elongated spermatids and mature sperm (Fig. 2B). However, the transcription of *WDR64* was hardly detected in macrophages or Sertoli cells (Fig. 2B). Next, according to the single-cell RNA sequencing datasets from the human epididymis published by Leir et al. [29], we analyzed the transcription of *WDR64* in the epididymis and found that *WDR64* was enriched in sperm but barely expressed in other epididymal cells (principal, apical, narrow, stromal, immune and clear cells) (Fig. 2C). These results indicate an important role of *WDR64* in germ cells.

3.3. *Wdr64* expression during murine testis development

To validate the expression profile of *Wdr64* during murine testis development, we detected the expression of *Wdr64* mRNA in different organs of adult mice by RT–qPCR, and the results revealed that *Wdr64* mRNA abundantly expressed in the testis but almost undetectable in the heart, liver, spleen, lung, kidney, epididymis, ovary, brain and muscle (Fig. 3A). The mouse WDR64 protein consists of 1084 amino acids and the theoretical molecular weight is 124 kDa. To verify this result, we constructed a recombinant *Wdr64* plasmid with Flag tag. The pLVX-Flag-Wdr64 recombinant plasmid was transfected into HEK293T cells, and the overexpression of WDR64 was detected by Western blotting with an anti-Flag antibody. The results revealed that the specific band of WDR64 was

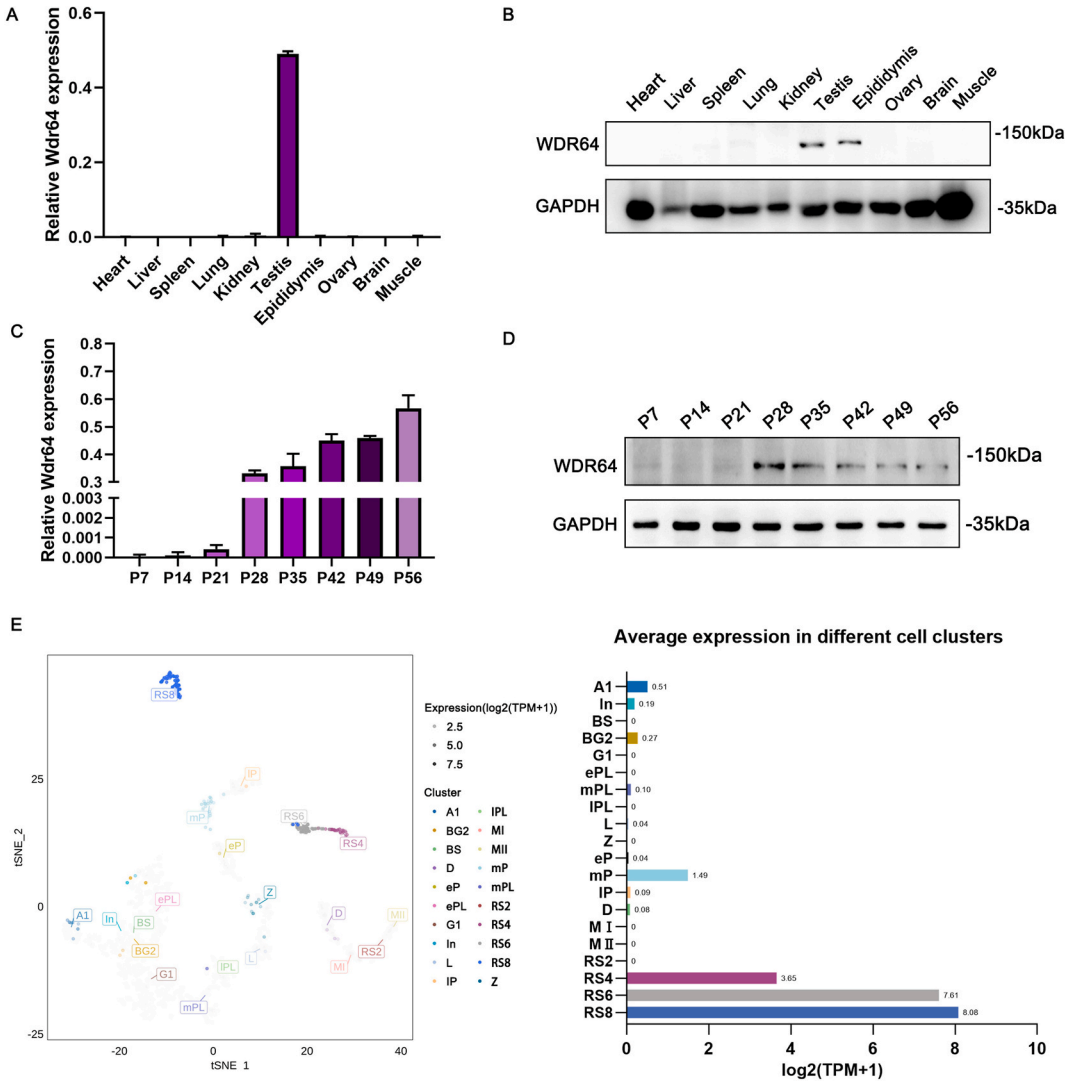

Fig. 3. Expression pattern *Wdr64* in mice. (A) RT–qPCR analysis of *Wdr64* mRNA expression in the heart, liver, spleen, lung, kidney, testis, epididymis, ovary, brain and muscle of adult mice (mean ± SD, n = 3). (B) Expression analysis of the WDR64 protein in different organs of adult mice by Western blot. (C) RT–qPCR analysis of *Wdr64* mRNA expression in different developmental stages of mouse testes (mean ± SD, n = 3). (D) Expression analysis of WDR64 protein in different developmental stages of mouse testes by Western blot. (E) Analysis of *Wdr64* expression in the single-cell RNA dataset of mouse testis samples published by Chen et al. [30].

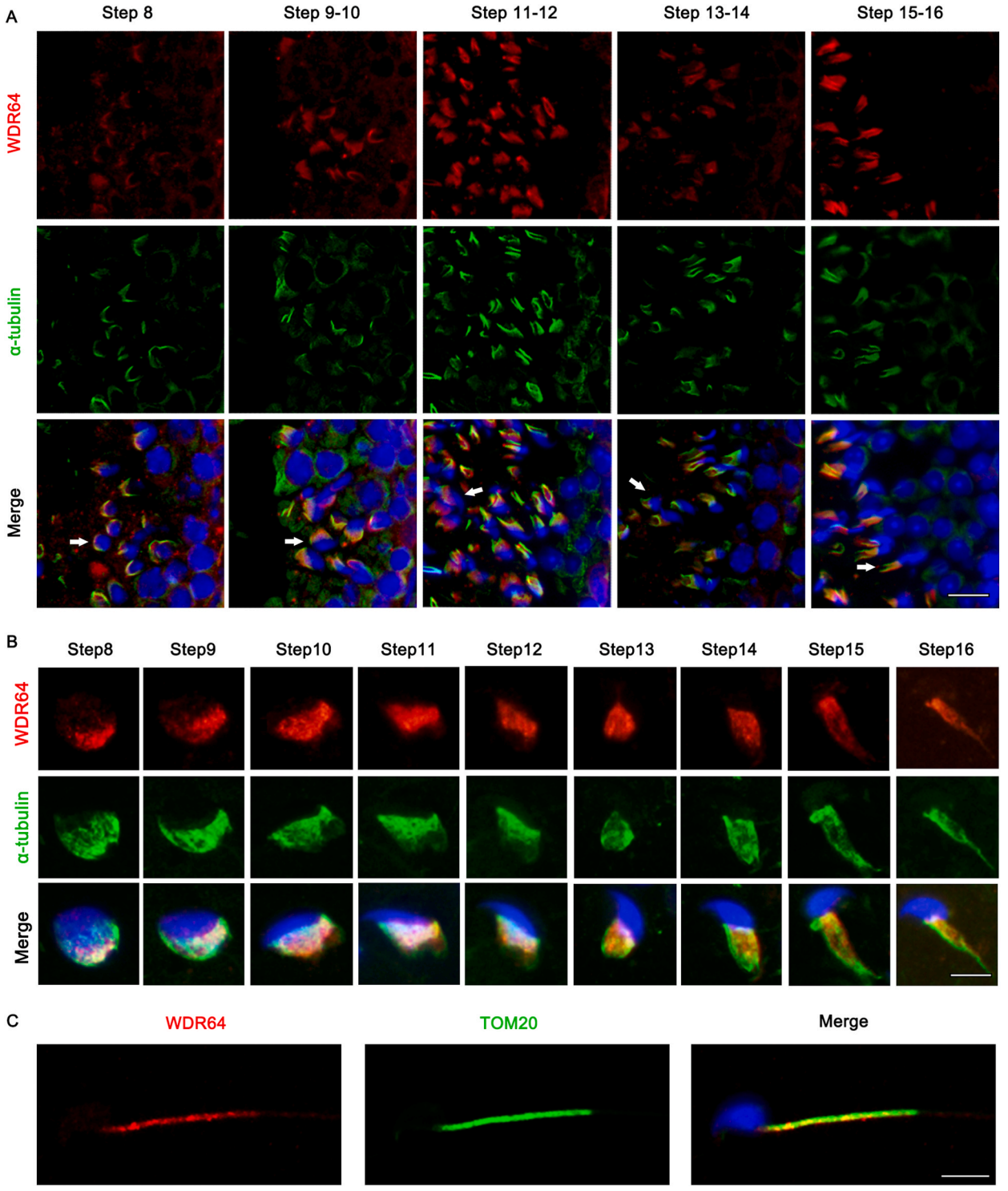

Fig. 4. Dynamic expression of WDR64 during spermiogenesis in mice. (A) Immunofluorescence analysis of testis sections stained with WDR64 (red), α-tubulin (green) and DAPI (blue). Bars: 10 μm. (B) Spermatids of different developmental steps isolated from adult mouse testes were stained with anti-WDR64 (red), anti-α-tubulin (green) and DAPI (blue). Bars: 5 μm. (C) Immunofluorescence analysis of epididymal spermatozoa stained with WDR64 (red), TOM20 (green), and DAPI (blue). Bars: 5 μm.

approximately 124 kDa, which was consistent with the calculated molecular weight (Supplementary Fig. S2). Next, we detected the expression of WDR64 protein in different organs of adult mice and Western blot results revealed that the WDR64 protein was detected in testes and epididymides (Fig. 3B), indicating that WDR64 may play a potentially important role in spermatogenesis. Further, we evaluated the changes in *Wdr64* mRNA expression levels in mouse testes by RT−qPCR and Western blotting, and the results revealed that *Wdr64* mRNA and WDR64 protein were weakly expressed at postnatal Day 7, with expression increasing substantially at postnatal Day 28 and being maintained high levels thereafter (Fig. 3C and D), which corresponded to the process of spermatogenesis. Analyses of the single-cell RNA sequencing datasets of mouse testes and epididymides published by Chen et al. and Shi et al. [30,31] further confirmed that *Wdr64* mRNA was predominantly expressed in postmeiotic germ cells and spermatozoa in the epididymis (Fig. 3E and Supplementary Fig. S1B), which was consistent with its high expression beginning at postnatal Day 28 in mice. These results revealed that the *Wdr64* gene is highly expressed in testis and strictly regulated by development.

3.4. Localization of WDR64 during spermiogenesis

To explore the distribution of WDR64, we performed immunofluorescence in mouse testis sections. We found that WDR64 was weakly expressed in the cytoplasm of spermatocytes and early round spermatids, and was strongly detectable in the posterior pole of late round spermatids and elongating spermatids (steps 8–16), where it colocalized with α-tubulin but was not distributed in the acrosome labeled by PNA (Fig. 4A and Supplementary Fig. S3). Because *Wdr64* is expressed mainly during spermiogenesis, we focused on the localization of WDR64 in the spermatid development stage to explore its possible biological function (Fig. 4B). Specifically, at the time of the appearance of the manchette in step 8, WDR64 strongly aggregated in the posterior pole of the round spermatids and was distributed in the manchette in subsequent steps. When the manchette disappeared, WDR64 migrated to the flagella of the spermatids at steps 15–16. In epididymal spermatozoa, WDR64 colocalized with TOM20, suggesting that WDR64 was located in the midpiece of the flagellum (Fig. 4C). These results revealed that WDR64 was located in the manchette and flagellum during spermiogenesis, suggesting that Wdr64 is a component of the spermatozoa flagellum.

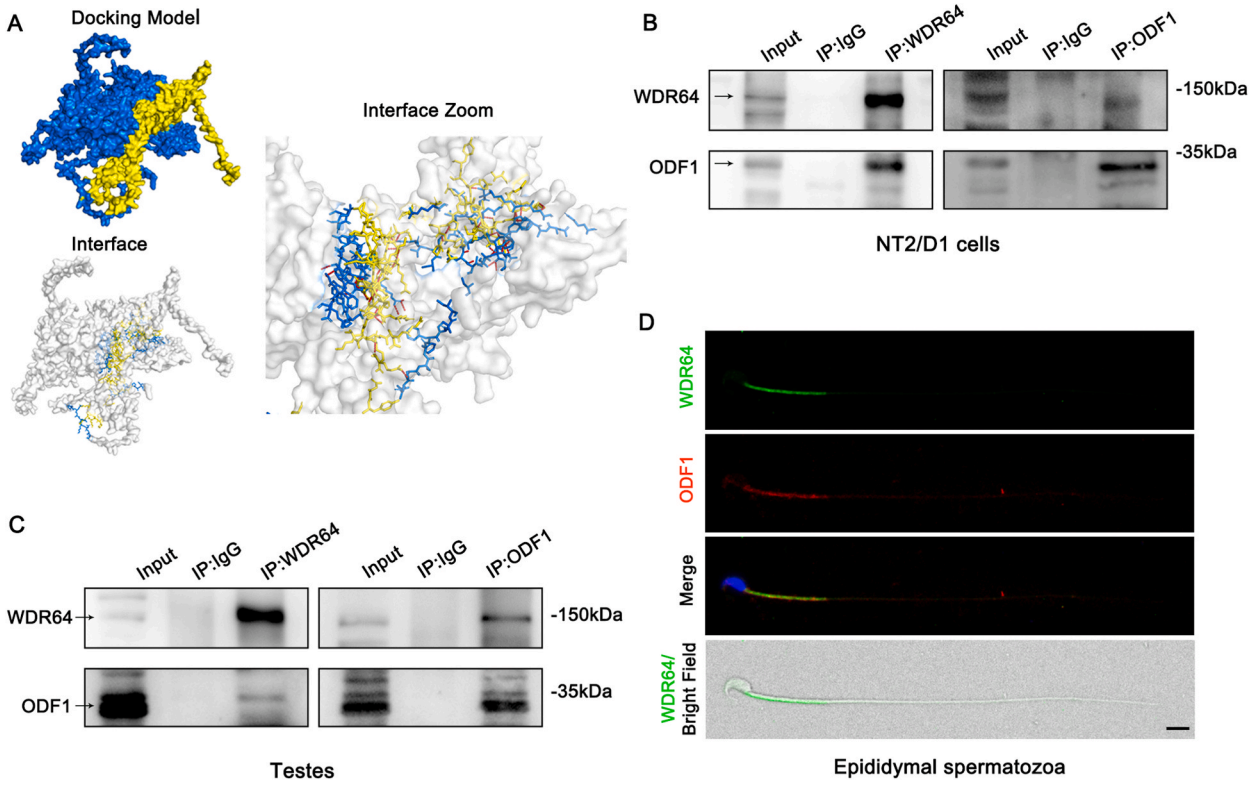

Fig. 5. WDR64 interacted with ODF1 to form a complex localized in the sperm flagella. (A) Surface diagram of the protein−protein docking model and the interfacing residues between WDR64 and ODF1 protein (WDR64, blue; ODF1, yellow; hydrogen bond and salt bridge interaction, dotted line). (B)Interaction between WDR64 and ODF1 in NT2/D1 cells was assessed by co-IP. Input proteins and normal IgG pulldowns were used as positive and negative controls, respectively. (C) Interaction between WDR64 and ODF1 in the testes of wild-type male mice was assessed by co-IP. (D) WDR64 and ODF1 in epididymal sperm were colocalized by immunofluorescence staining with antibodies against theWDR64 (green) and ODF1 (red). Bars: 5 μm.

3.5. WDR64 interacts with ODF1 to form a complex

To explore the molecular mechanisms of WDR64 in spermatogenesis, we investigated the WDR64 interacting proteins. We found that WDR64 was highly expressed in NT2/D1 cells (Supplementary Fig. S4) and co-IP was subsequently performed using WDR64 antibodies. Mass spectrometry was used to identify the protein partners that interact with WDR64. The results revealed that WDR64 was pulled down and 15 unique peptides of outer dense fiber 1(ODF1) were detected in the immunoprecipitates (Supplementary Fig. S5).

To verify their specific relationship, we performed rigid protein–protein docking between WDR64 and ODF1. As shown in Fig. 5A and Supplemental Table S2, WDR64 and ODF1 formed hydrogen bonds, which were mainly distributed in WD6 and WD9 domains of WDR64 and ACD_HspB10 domain of ODF1, revealing that the proteins WDR64 and ODF1 formed a stable protein docking model. We

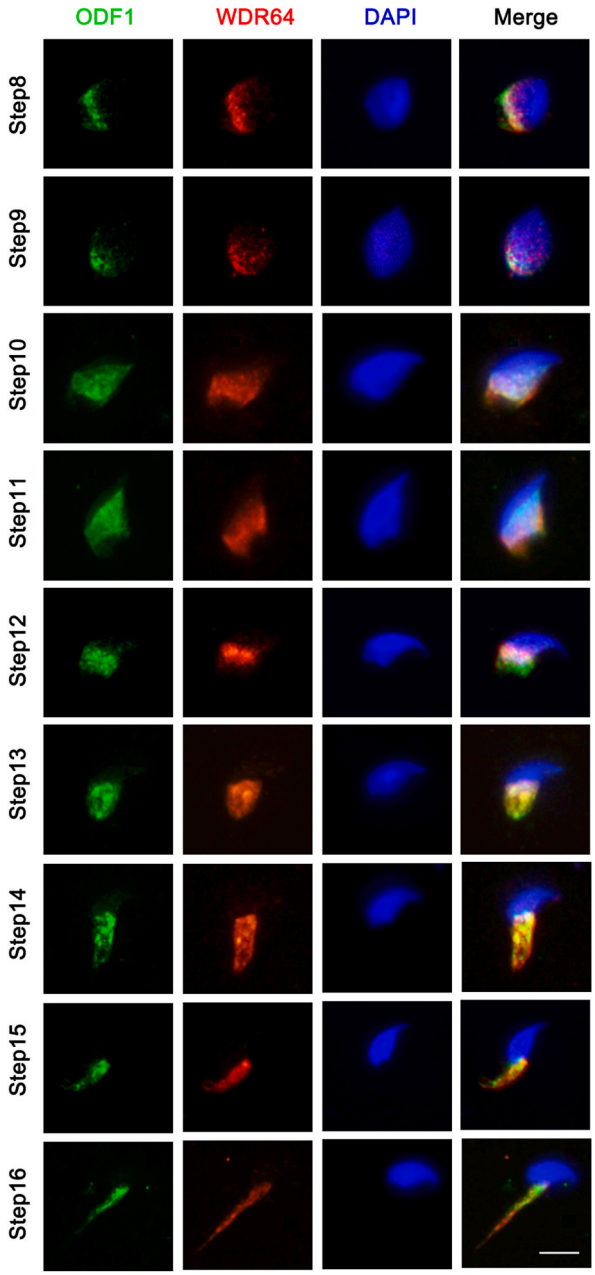

Fig. 6. Expression of the WDR64/ODF1 complex at different stages of spermatid development in mice. Immunofluorescence staining of elongating spermatids (steps 8–16) was performed with antibodies against WDR64 (red) and ODF1 (green). The nuclei were stained with DAPI (blue). Bars: 5 μm.

next visualized the interaction between WDR64 and ODF1 in a co-IP assay. NT2/D1 cells were obtained and the assay was performed using antibodies against WDR64 and ODF1 antibodies. In the immunoprecipitates of the WDR64 antibodies, both the ODF1 and WDR64 bands were detected, and in the reverse immunoprecipitates of the ODF1 antibodies, the ODF1 and WDR64 bands were also detected. (Fig. 5B). Furthermore, we performed Co-IP on mouse testicular proteins to confirm their actual interaction and the results revealed that ODF1 and WDR64 were immunoprecipitated by antibodies against WDR64 and ODF1, respectively (Fig. 5C).

ODF1 is one of the most important components of the sperm flagellum. The sperm flagellum has an ultrastructurally comparable axonemal structure, but the sperm tail also contains accessory structures: the mitochondrial sheath, fibrous sheath and outer dense fibers. As the main component of the ODFs, ODF1 protects the sperm tail against shear forces [46]. Previous studies revealed that the percentage of ODF defects was greater in asthenozoospermic samples than in control samples and that the expression levels of ODF1 were frequently downregulated in asthenozoospermic samples [47]. It is highly correlated with dynamic changes in manchettes during sperm development and is localized in the tail of mature sperm [48]. We next investigated the localization of WDR64 and ODF1 in mouse spermatozoa and immunofluorescence showed that the red signal of ODF1 colocalized with the green signal of WDR64 in the midpiece of the sperm flagellum (Fig. 5D). These results revealed that WDR64 interacted with ODF1 to form a complex at the sperm flagellum.

3.6. Dynamic localization of the WDR64/ODF1 complex during spermiogenesis

To explore the function of the WDR64/ODF1 complex, we observed the dynamic changes in the complex during spermiogenesis. The results of the immunofluorescence assay revealed that WDR64 always colocalized with ODF1 at steps 8–16 of spermiogenesis (Fig. 6). At step 8, the WDR64/ODF1 complex was distributed posterior to the nucleus. The complex then extended to form a skirt-like structure concurrent with nuclear condensation as the spermatids progressed from steps 9–14. Finally at steps 15–16, the WDR64/ODF1 complex migrated to the spermatid flagellum after the disassembly of the manchette. These data revealed that WDR64 colocalized with ODF1 in spermiogenesis and the dynamic localization pattern of the WDR64/ODF1 complex was consistent with that of the manchette [49].

4. Discussion

The process of spermatogenesis is accompanied by the phasic regulation of many genes, especially testis-specific genes [50]. In this study, we identified a novel testis-specific gene, *WDR64*, which was weakly expressed at postnatal Day 7, dramatically increased at postnatal Day 28 and maintained at high levels thereafter. Immunofluorescence analysis revealed that WDR64 was expressed in male germ cells, especially in postmeiotic germ cells. Further, we demonstrated that WDR64 interacted with ODF1 to form a complex both *in vitro* and *in vivo*. WDR64 colocalized with the ODF1 at the manchette in elongating spermatids and the midpiece of the flagellum in spermatozoa. These data provide a primary understanding of WDR64 in spermatogenesis.

WDR64 belongs to WDR protein family. WDR proteins are well-known for their protein interacting capacity and play a crucial role in spermatogenesis [51]. For example, WDR62 is involved in male germ cell meiosis [44]; DCAF8 and WDR12 are involved in sperm head shaping [14,15]; WDR38 is associated with spermatid acrosome biogenesis [22]; and, CFAP43, CFAP44, CFAP251, WDR63 and WDR87 are critical for sperm flagellum formation [17,19–21,52]. After screening of WDR genes enriched in the testis, we found that *WDR64* was a novel potentially testis-specific expressed gene that has not been previously reported. Subsequent RT-PCR and Western blot showed that *Wdr64* was specifically expressed in testis and was strictly regulated by development. Further, immunofluorescence of testicular sections revealed that *Wdr64* was strongly expressed in developing spermatids, indicating that WDR64 may be involved in spermiogenesis.

Spermiogenesis is the last phase of spermatogenesis, where the nucleus is remodeled with chromatin condensation, and the acrosome and sperm tail are formed. The manchette is a critical and transient structure that surrounds the elongating spermatid head and exists only during spermatid elongation [46]. It first occurs in step 8 spermatids forming a microtubular platform between the perinuclear ring and axoneme [53], and then disassembles until steps 13–14 spermatids prior to the mid-piece of flagellum formation [46]. Current studies demonstrate that the temporal and spatial properties of the manchette facilitate the transport of accessory structural proteins to the sperm tail. Intramanchette transport (IMT) and intraflagellar transport (IFT) are the mechanisms that store and transport proteins and protein complexes to developing flagella [54,55]. In fact, many components of sperm flagella can be temporarily localized in manchette, and the affected IFT and IMT lead to defects in the transport of flagellar proteins [46]. We noticed that WDR64 colocalized with α-tubulin, the microtubules of the manchette. In the IP-MS protein list, α-tubulin and β-tubulin were also detected in addition to ODF1, indicating that WDR64 is a component of the manchette.

The WDR64/ODF1 complex changed in line with the changes in the manchette at steps 8–14 and moved to the developing flagellum at steps 15–16. It has been reported that ODFs are transported through the manchette during spermiogenesis and elongate in a proximal to distal direction [46]. In IFT88 mutant mice, ODF proteins accumulate in the manchette indicating that IMT is required for their transport [56]. Several components of ODFs have been identified and the main structural and only sperm-specific protein is ODF1 [46]. Depletion of ODF1 affects the formation of ODFs, the mitochondrial sheath (MS) and the connecting piece, leading to detached sperm heads and male infertility [57,58]. A study of patients with asthenozoospermia demonstrated that ODF defects were more common in asthenozoospermic samples than in control samples, and the expression level of ODF1 was also downregulated in these samples, revealing the function of ODF1 in sperm motility [47]. Yang et al. [59] performed state-of-the-art 4D-quantitative proteomics analysis to compare protein profiles between control and asthenozoospermic samples, and we noted that both WDR64 and ODF1 were downregulated in asthenozoospermic samples in the protein lists, indicating that the WDR64/ODF1 complex is associated with sperm

motility. Recently, we generated *Wdr64* knockout mice and found that the deletion of *Wdr64* led to decreased sperm motility (data not shown). Owing to the irreplaceable role of ODF1 in spermatogenesis, we suppose that the WDR64/ODF1 complex is important for sperm motility.

Taken together, we identified a novel testis-specific gene, *WDR64*, and described its expression pattern in spermatogenesis. The expression of WDR64 mainly distributed in postmeiotic germ cells and was strictly regulated by development. The WDR64 interacted with the ODF1 to form a complex colocalizing at the manchette in elongating spermatids and the midpiece of the flagellum in spermatozoa. Our findings provide the first evidence for a putative association of WDR64 function. Further studies are needed to identify *WDR64* mutations in patients with male infertility, and perform *Wdr64* gene knockout in animal models to verify its detail function and potential molecular mechanism.

Funding

This project was funded by the Natural Science Foundation of Hunan Province, China (Grant No. 2023JJ30850) and the Changsha Natural Science Foundation, Hunan, China (kq2208354).

Ethics statement

For the animal experiments, the protocols of this study were approved by the Institutional Animal Care and Use Committee (IACUC) of Central South University (Approval number: CSU-2022-0559).

Data availability statement

The data needed to support the findings in this study are available in the paper and/or the supplementary materials. The raw MS data will be made available upon request. The programs PyMOL (https://pymol.org/2/), Clustal (http://www.clustal.org/), MAGEX (https://www.megasoftware.net/), ESPript 3.0 (https://espript.ibcp.fr/ESPript/cgi-bin/ESPript.cgi), Human Protein Atlas (https://www.proteinatlas.org/), the Sperm Maturation Database (http://bio-add.org/SperMD), GRAMM-X (http://gramm.compbio.ku.edu/) and PDBePISA (https://www.ebi.ac.uk/pdbe/pisa/) are publicly and freely available.

CRediT authorship contribution statement

Yunfei Zhang: Writing – original draft, Visualization, Methodology, Investigation, Formal analysis, Data curation, Conceptualization. **Xiaowei Xing:** Writing – review & editing, Funding acquisition, Conceptualization. **Lihua Huang:** Writing – review & editing. **Yuyan Su:** Validation, Methodology. **Gang Liu:** Visualization, Validation, Formal analysis. **Xinxing Zhang:** Methodology. **Youbo Yang:** Writing – review & editing, Supervision, Project administration, Investigation, Conceptualization.

Declaration of competing interest

The authors declare that they have no known competing financial interests or personal relationships that could have appeared to influence the work reported in this paper.

Appendix A. Supplementary data

Supplementary data to this article can be found online at https://doi.org/10.1016/j.heliyon.2024.e38263.

References

[1] M.L. Eisenberg, S.C. Esteves, D.J. Lamb, J.M. Hotaling, A. Giwercman, K. Hwang, Y.S. Cheng, Male infertility, Nat. Rev. Dis. Prim. 9 (2023) 49, https://doi.org/10.1038/s41572-023-00459-w.
[2] O. Zalewska, K. Wszołek, M. Pięt, M. Wilczak, K. Chmaj-Wierzchowska, Women's awareness of reproductive health, Medicina (Kaunas) 60 (2024) 158, https://doi.org/10.3390/medicina60010158.
[3] S.Y. Jiao, Y.H. Yang, S.R. Chen, Molecular genetics of infertility: loss-of-function mutations in humans and corresponding knockout/mutated mice, Hum. Reprod. Update 27 (2021) 154–189, https://doi.org/10.1093/humupd/dmaa034.
[4] C. Tu, W. Wang, T. Hu, G. Lu, G. Lin, Y.Q. Tan, Genetic underpinnings of asthenozoospermia, Best Pract. Res. Clin. Endocrinol. Metabol. 34 (2020) 101472, https://doi.org/10.1016/j.beem.2020.101472.
[5] C. Krausz, A. Riera-Escamilla, Genetics of male infertility, Nat. Rev. Urol. 15 (2018) 369–384, https://doi.org/10.1038/s41585-018-0003-3.
[6] C. Xu, J. Min, Structure and function of WD40 domain proteins, PROTEIN CELL 2 (2011) 202–214, https://doi.org/10.1007/s13238-011-1018-1.
[7] D. Li, R. Roberts, WD-repeat proteins: structure characteristics, biological function, and their involvement in human diseases, Cell. Mol. Life Sci. 58 (2001) 2085–2097, https://doi.org/10.1007/pl00000838.
[8] M. Schapira, M. Tyers, M. Torrent, C.H. Arrowsmith, WD40 repeat domain proteins: a novel target class? Nat. Rev. Drug Discov. 16 (2017) 773–786, https://doi.org/10.1038/nrd.2017.179.
[9] Y. Kim, S.H. Kim, WD40-Repeat proteins in ciliopathies and congenital disorders of endocrine system, Endocrinol Metab (Seoul) 35 (2020) 494–506, https://doi.org/10.3803/EnM.2020.302.

[10] Z. Zhang, Q. Zhu, WD repeat and HMG box DNA binding protein 1: an oncoprotein at the hub of tumorigenesis and a novel therapeutic target, Int. J. Mol. Sci. 24 (2023), https://doi.org/10.3390/ijms241512494.
[11] Y. Zhou, Y. Qin, Y. Qin, B. Xu, T. Guo, H. Ke, M. Chen, L. Zhang, F. Han, Y. Li, M. Chen, A. Behrens, Y. Wang, Z. Xu, Z.J. Chen, F. Gao, Wdr62 is involved in female meiotic initiation via activating JNK signaling and associated with POI in humans, PLoS Genet. 14 (2018) e1007463, https://doi.org/10.1371/journal.pgen.1007463.
[12] Y.S. Wang, C. Chen, M.J. Ahmad, F. Chen, Z.M. Ding, S.J. Yang, Y.W. Chen, Z.Q. Duan, M. Liu, A.X. Liang, C.J. He, G.H. Hua, L.J. Huo, WDR62 regulates mouse oocyte meiotic maturation related to p-JNK and H3K9 trimethylation, Int. J. Biochem. Cell Biol. 144 (2022) 106169, https://doi.org/10.1016/j.biocel.2022.106169.
[13] Y. Qin, Y. Zhou, Z. Shen, B. Xu, M. Chen, Y. Li, M. Chen, A. Behrens, J. Zhou, X. Qi, W. Meng, Y. Wang, F. Gao, WDR62 is involved in spindle assembly by interacting with CEP170 in spermatogenesis, Development 146 (2019), https://doi.org/10.1242/dev.174128.
[14] X. Zhang, Z. Xia, X. Lv, D. Li, M. Liu, R. Zhang, T. Ji, P. Liu, R. Ren, DDB1- and CUL4-associated factor 8 plays a critical role in spermatogenesis, Front. Med. 15 (2021) 302–312, https://doi.org/10.1007/s11684-021-0851-8.
[15] J. Hua, L. Guo, Y. Yao, W. Hu, Y.Y. Wan, B. Xu, Biallelic mutations in WDR12 are associated with male infertility with tapered-head sperm, Asian J. Androl. 25 (2023) 398–403, https://doi.org/10.4103/aja202269.
[16] C. Coutton, A.S. Vargas, A. Amiri-Yekta, Z.E. Kherraf, M.S. Ben, P. Le Tanno, C. Wambergue-Legrand, T. Karaouzène, G. Martinez, S. Crouzy, A. Daneshipour, S. H. Hosseini, V. Mitchell, L. Halouani, O. Marrakchi, M. Makni, H. Latrous, M. Kharouf, J.F. Deleuze, A. Boland, S. Hennebicq, V. Satre, P.S. Jouk, N. Thierry-Mieg, B. Conne, D. Dacheux, N. Landrein, A. Schmitt, L. Stouvenel, P. Lorès, K.E. El, S.P. Bottari, J. Fauré, J.P. Wolf, K. Pernet-Gallay, J. Escoffier, H. Gourabi, D. R. Robinson, S. Nef, E. Dulioust, R. Zouari, M. Bonhivers, A. Touré, C. Arnoult, P.F. Ray, Mutations in CFAP43 and CFAP44 cause male infertility and flagellum defects in Trypanosoma and human, Nat. Commun. 9 (2018) 686, https://doi.org/10.1038/s41467-017-02792-7.
[17] S. Tang, X. Wang, W. Li, X. Yang, Z. Li, W. Liu, C. Li, Z. Zhu, L. Wang, J. Wang, L. Zhang, X. Sun, E. Zhi, H. Wang, H. Li, L. Jin, Y. Luo, J. Wang, S. Yang, F. Zhang, Biallelic mutations in CFAP43 and CFAP44 cause male infertility with multiple morphological abnormalities of the sperm flagella, Am. J. Hum. Genet. 100 (2017) 854–864, https://doi.org/10.1016/j.ajhg.2017.04.012.
[18] Z.E. Kherraf, A. Amiri-Yekta, D. Dacheux, T. Karaouzène, C. Coutton, M. Christou-Kent, G. Martinez, N. Landrein, P. Le Tanno, B.M.S. Fourati, L. Halouani, O. Marrakchi, M. Makni, H. Latrous, M. Kharouf, K. Pernet-Gallay, H. Gourabi, D.R. Robinson, S. Crouzy, M. Blum, N. Thierry-Mieg, A. Touré, R. Zouari, C. Arnoult, M. Bonhivers, P.F. Ray, A homozygous ancestral SVA-insertion-mediated deletion in WDR66 induces multiple morphological abnormalities of the sperm flagellum and male infertility, Am. J. Hum. Genet. 103 (2018) 400–412, https://doi.org/10.1016/j.ajhg.2018.07.014.
[19] W. Li, X. He, S. Yang, C. Liu, H. Wu, W. Liu, M. Lv, D. Tang, J. Tan, S. Tang, Y. Chen, J. Wang, Z. Zhang, H. Wang, L. Jin, F. Zhang, Y. Cao, Biallelic mutations of CFAP251 cause sperm flagellar defects and human male infertility, J. Hum. Genet. 64 (2019) 49–54, https://doi.org/10.1038/s10038-018-0520-1.
[20] S. Lu, Y. Gu, Y. Wu, S. Yang, C. Li, L. Meng, W. Yuan, T. Jiang, X. Zhang, Y. Li, C. Wang, M. Liu, L. Ye, X. Guo, H. Shen, X. Yang, Y. Tan, Z. Hu, Bi-allelic variants in human WDR63 cause male infertility via abnormal inner dynein arms assembly, CELL DISCOV 7 (2021) 110, https://doi.org/10.1038/s41421-021-00327-5.
[21] H.Q. Liao, Z.Y. Guo, L.H. Huang, G. Liu, J.F. Lu, Y.F. Zhang, X.W. Xing, WDR87 interacts with CFAP47 protein in the middle piece of spermatozoa flagella to participate in sperm tail assembly, Mol. Hum. Reprod. 29 (2022), https://doi.org/10.1093/molehr/gaac042.
[22] Q. Gao, G. Liu, L. Huang, Y. Zhang, X. Zhang, X. Song, X. Xing, WDR38, a novel equatorial segment protein, interacts with the GTPase protein RAB19 and Golgi protein GM130 to play roles in acrosome biogenesis, Acta Biochim. Biophys. Sin. 55 (2023) 1561–1570, https://doi.org/10.3724/abbs.2023126.
[23] J. Jumper, R. Evans, A. Pritzel, T. Green, M. Figurnov, O. Ronneberger, K. Tunyasuvunakool, R. Bates, A. Žídek, A. Potapenko, A. Bridgland, C. Meyer, S. Kohl, A.J. Ballard, A. Cowie, B. Romera-Paredes, S. Nikolov, R. Jain, J. Adler, T. Back, S. Petersen, D. Reiman, E. Clancy, M. Zielinski, M. Steinegger, M. Pacholska, T. Berghammer, S. Bodenstein, D. Silver, O. Vinyals, A.W. Senior, K. Kavukcuoglu, P. Kohli, D. Hassabis, Highly accurate protein structure prediction with AlphaFold, Nature 596 (2021) 583–589, https://doi.org/10.1038/s41586-021-03819-2.
[24] K. Tamura, G. Stecher, S. Kumar, MEGA11: molecular evolutionary genetics analysis version 11, Mol. Biol. Evol. 38 (2021) 3022–3027, https://doi.org/10.1093/molbev/msab120.
[25] M.A. Larkin, G. Blackshields, N.P. Brown, R. Chenna, P.A. McGettigan, H. McWilliam, F. Valentin, I.M. Wallace, A. Wilm, R. Lopez, J.D. Thompson, T.J. Gibson, D.G. Higgins, Clustal W and clustal X version 2.0, Bioinformatics 23 (2007) 2947–2948, https://doi.org/10.1093/bioinformatics/btm404.
[26] Y. Li, Q. Li, L. Wu, H. Wang, H. Shi, C. Yang, Y. Gu, J. Li, Z. Ji, SperMD: the expression atlas of sperm maturation, BMC Bioinf. 25 (2024) 29, https://doi.org/10.1186/s12859-024-05631-x.
[27] J. Guo, E.J. Grow, H. Mlcochova, G.J. Maher, C. Lindskog, X. Nie, Y. Guo, Y. Takei, J. Yun, L. Cai, R. Kim, D.T. Carrell, A. Goriely, J.M. Hotaling, B.R. Cairns, The adult human testis transcriptional cell atlas, Cell Res. 28 (2018) 1141–1157, https://doi.org/10.1038/s41422-018-0099-2.
[28] J. Guo, X. Nie, M. Giebler, H. Mlcochova, Y. Wang, E.J. Grow, R. Kim, M. Tharmalingam, G. Matilionyte, C. Lindskog, D.T. Carrell, R.T. Mitchell, A. Goriely, J. M. Hotaling, B.R. Cairns, The dynamic transcriptional cell atlas of testis development during human puberty, Cell Stem Cell 26 (2020) 262–276, https://doi.org/10.1016/j.stem.2019.12.005.
[29] S.H. Leir, S. Yin, J.L. Kerschner, W. Cosme, A. Harris, An atlas of human proximal epididymis reveals cell-specific functions and distinct roles for CFTR, Life Sci. Alliance 3 (2020) e202000744, https://doi.org/10.26508/lsa.202000744.
[30] Y. Chen, Y. Zheng, Y. Gao, Z. Lin, S. Yang, T. Wang, Q. Wang, N. Xie, R. Hua, M. Liu, J. Sha, M.D. Griswold, J. Li, F. Tang, M.H. Tong, Single-cell RNA-seq uncovers dynamic processes and critical regulators in mouse spermatogenesis, Cell Res. 28 (2018) 879–896, https://doi.org/10.1038/s41422-018-0074-y.
[31] J. Shi, K.L. Fok, P. Dai, F. Qiao, M. Zhang, H. Liu, M. Sang, M. Ye, Y. Liu, Y. Zhou, C. Wang, F. Sun, G. Xie, H. Chen, Spatio-temporal landscape of mouse epididymal cells and specific mitochondria-rich segments defined by large-scale single-cell RNA-seq, CELL DISCOV 7 (2021) 34, https://doi.org/10.1038/s41421-021-00260-7.
[32] Y. Chang, X. Wang, Y. Xu, L. Yang, Q. Qian, S. Ju, Y. Chen, S. Chen, N. Qin, Z. Ma, J. Dai, H. Ma, G. Jin, E. Zhang, C. Wang, Z. Hu, Comprehensive characterization of cancer-testis genes in testicular germ cell tumor, Cancer Med. 8 (2019) 3511–3519, https://doi.org/10.1002/cam4.2223.
[33] B.J. Houston, A.M. Lopes, M. Laan, L. Nagirnaja, A.E. O'Connor, D.J. Merriner, J. Nguyen, M. Punab, A. Riera-Escamilla, C. Krausz, K.I. Aston, D.F. Conrad, M. K. O'Bryan, DDB1- and CUL4-associated factor 12-like protein 1 (Dcaf12l1) is not essential for male fertility in mice, Dev. Biol. 490 (2022) 66–72, https://doi.org/10.1016/j.ydbio.2022.07.006.
[34] D. Ma, J. Yang, Y. Wang, X. Huang, G. Du, L. Zhou, Whole exome sequencing identified genetic variations in Chinese hemangioblastoma patients, Am. J. Med. Genet. A 173 (2017) 2605–2613, https://doi.org/10.1002/ajmg.a.38350.
[35] F. Liu, Q. Han, T. Zhang, F. Chang, J. Deng, X. Huang, W. Wang, Y. Xu, Q. Li, L. Xu, B. Zhang, W. Li, L. Li, Y. Su, Y. Li, G. Shao, CRL4-DCAF8L1 regulates BRCA1 and BARD1 protein stability, Int. J. Biol. Sci. 18 (2022) 1434–1450, https://doi.org/10.7150/ijbs.57178.
[36] Y. Tian, E. Arai, S. Makiuchi, N. Tsuda, J. Kuramoto, K. Ohara, Y. Takahashi, N. Ito, H. Ojima, N. Hiraoka, M. Gotoh, T. Yoshida, Y. Kanai, Aberrant DNA methylation results in altered gene expression in non-alcoholic steatohepatitis-related hepatocellular carcinomas, J. Cancer Res. Clin. Oncol. 146 (2020) 2461–2477, https://doi.org/10.1007/s00432-020-03298-4.
[37] T.H. Beaty, M.A. Taub, A.F. Scott, J.C. Murray, M.L. Marazita, H. Schwender, M.M. Parker, J.B. Hetmanski, P. Balakrishnan, M.A. Mansilla, E. Mangold, K. U. Ludwig, M.M. Noethen, M. Rubini, N. Elcioglu, I. Ruczinski, Confirming genes influencing risk to cleft lip with/without cleft palate in a case-parent trio study, Hum. Genet. 132 (2013) 771–781, https://doi.org/10.1007/s00439-013-1283-6.
[38] N.N. Feng, X.Y. Du, Y.S. Zhang, Z.K. Jiao, X.H. Wu, B.M. Yang, Overweight/obesity-related transcriptomic signature as a correlate of clinical outcome, immune microenvironment, and treatment response in hepatocellular carcinoma, Front. Endocrinol. 13 (2022) 1061091, https://doi.org/10.3389/fendo.2022.1061091.
[39] Y. Li, S. Liu, Y.T. Wang, H. Min, D. Adi, X.M. Li, Y.N. Yang, Z.Y. Fu, Y.T. Ma, TBL2 methylation is associated with hyper-low-density lipoprotein cholesterolemia: a case-control study, Lipids Health Dis. 19 (2020) 186, https://doi.org/10.1186/s12944-020-01359-8.
[40] M. Yang, M. Liu, Z. Wang, C. Zhang, Mice lacking DCAF2 in placenta die at the gastrulation stage, Cell Tissue Res. 389 (2022) 559–572, https://doi.org/10.1007/s00441-022-03655-4.
[41] Y.W. Xu, L.R. Cao, M. Wang, Y. Xu, X. Wu, J. Liu, C. Tong, H.Y. Fan, Maternal DCAF2 is crucial for maintenance of genome stability during the first cell cycle in mice, J. Cell Sci. 130 (2017) 3297–3307, https://doi.org/10.1242/jcs.206664.

[42] T. Kang, Y. Wan, Z. Zhang, K.M. Chan, Lrwd1 impacts cell proliferation and the silencing of repetitive DNA elements, Genesis 60 (2022) e23475, https://doi.org/10.1002/dvg.23475.
[43] Y. Zhi, X. Zhou, J. Yu, L. Yuan, H. Zhang, D. Ng, Z. Xu, D. Xu, Pathophysiological significance of WDR62 and JNK signaling in human diseases, Front. Cell Dev. Biol. 9 (2021) 640753, https://doi.org/10.3389/fcell.2021.640753.
[44] U.Y. Ho, C.A. Feng, Y.Y. Yeap, A.L. Bain, Z. Wei, B. Shohayeb, M.E. Reichelt, H. Homer, K.K. Khanna, J. Bowles, D. Ng, WDR62 is required for centriole duplication in spermatogenesis and manchette removal in spermiogenesis, Commun. Biol. 4 (2021) 645, https://doi.org/10.1038/s42003-021-02171-5.
[45] A.L. Richards, G. Leonenko, J.T. Walters, D.H. Kavanagh, E.G. Rees, A. Evans, K.D. Chambert, J.L. Moran, J. Goldstein, B.M. Neale, S.A. McCarroll, A. J. Pocklington, P.A. Holmans, M.J. Owen, M.C. O'Donovan, Exome arrays capture polygenic rare variant contributions to schizophrenia, Hum. Mol. Genet. 25 (2016) 1001–1007, https://doi.org/10.1093/hmg/ddv620.
[46] M.S. Lehti, A. Sironen, Formation and function of the manchette and flagellum during spermatogenesis, Reproduction 151 (2016) R43–R54, https://doi.org/10.1530/REP-15-0310.
[47] W. Zhao, Z. Li, P. Ping, G. Wang, X. Yuan, F. Sun, Outer dense fibers stabilize the axoneme to maintain sperm motility, J. Cell Mol. Med. 22 (2018) 1755–1768, https://doi.org/10.1111/jcmm.13457.
[48] C.C. Tapia, S. Hoyer-Fender, CCDC42 localizes to manchette, HTCA and tail and interacts with ODF1 and ODF2 in the formation of the male germ cell cytoskeleton, Front. Cell Dev. Biol. 7 (2019) 151, https://doi.org/10.3389/fcell.2019.00151.
[49] C. Pleuger, M.S. Lehti, J.E. Dunleavy, D. Fietz, M.K. O'Bryan, Haploid male germ cells-the Grand Central Station of protein transport, Hum. Reprod. Update 26 (2020) 474–500, https://doi.org/10.1093/humupd/dmaa004.
[50] F.T. Neto, P.V. Bach, B.B. Najari, P.S. Li, M. Goldstein, Spermatogenesis in humans and its affecting factors, Semin. Cell Dev. Biol. 59 (2016) 10–26, https://doi.org/10.1016/j.semcdb.2016.04.009.
[51] B.P. Jain, S. Pandey, WD40 repeat proteins: signalling scaffold with diverse functions, Protein J. 37 (2018) 391–406, https://doi.org/10.1007/s10930-018-9785-7.
[52] H. Wu, W. Li, X. He, C. Liu, Y. Fang, F. Zhu, H. Jiang, W. Liu, B. Song, X. Wang, P. Zhou, Z. Wei, F. Zhang, Y. Cao, Novel CFAP43 andCFAP44 mutations cause male infertility with multiple morphological abnormalities of the sperm flagella (MMAF), Reprod. Biomed. Online 38 (2019) 769–778, https://doi.org/10.1016/j.rbmo.2018.
[53] L. O'Donnell, M.K. O'Bryan, Microtubules and spermatogenesis, Semin. Cell Dev. Biol. 30 (2014) 45–54, https://doi.org/10.1016/j.semcdb.2014.01.003.
[54] A.J. San, G.J. Pazour, G.B. Witman, Intraflagellar transport is essential for mammalian spermiogenesis but is absent in mature sperm, Mol. Biol. Cell 26 (2015) 4358–4372, https://doi.org/10.1091/mbc.E15-08-0578.
[55] A.L. Kierszenbaum, Intramanchette transport (IMT): managing the making of the spermatid head, centrosome, and tail, Mol. Reprod. Dev. 63 (2002) 1–4, https://doi.org/10.1002/mrd.10179.
[56] A.L. Kierszenbaum, E. Rivkin, L.L. Tres, B.K. Yoder, C.J. Haycraft, M. Bornens, R.M. Rios, GMAP210 and IFT88 are present in the spermatid golgi apparatus and participate in the development of the acrosome-acroplaxome complex, head-tail coupling apparatus and tail, Dev. Dynam. 240 (2011) 723–736, https://doi.org/10.1002/dvdy.22563.
[57] K. Yang, P. Grzmil, A. Meinhardt, S. Hoyer-Fender, Haplo-deficiency of ODF1/HSPB10 in mouse sperm causes relaxation of head-to-tail linkage, Reproduction 148 (2014) 499–506, https://doi.org/10.1530/REP-14-0370.
[58] K. Yang, A. Meinhardt, B. Zhang, P. Grzmil, I.M. Adham, S. Hoyer-Fender, The small heat shock protein ODF1/HSPB10 is essential for tight linkage of sperm head to tail and male fertility in mice, Mol. Cell Biol. 32 (2012) 216–225, https://doi.org/10.1128/MCB.06158-11.
[59] J. Yang, Q. Liu, B. Yu, B. Han, B. Yang, 4D-quantitative proteomics signature of asthenozoospermia and identification of extracellular matrix protein 1 as a novel biomarker for sperm motility, Mol Omics 18 (2022) 83–91, https://doi.org/10.1039/d1mo00257k.